arXiv:2412.00733v3 [cs.CV] 4 Jan 2025

Hallo3: Highly Dynamic and Realistic Portrait Image Animation with Diffusion Transformer Networks

Jiahao Cui[1], Hui Li[1], Yun Zhan[1], Hanlin Shang[1], Kaihui Cheng[1], Yuqi Ma[1], Shan Mu[1], Hang Zhou[2], Jingdong Wang[2], Siyu Zhu[1,3]
[1]Fudan University, [2]Baidu Inc, [3]Shanghai Academy of AI for Science

Abstract

Existing methodologies for animating portrait images face significant challenges, particularly in handling non-frontal perspectives, rendering dynamic objects around the portrait, and generating immersive, realistic backgrounds. In this paper, we introduce the first application of a pretrained transformer-based video generative model that demonstrates strong generalization capabilities and generates highly dynamic, realistic videos for portrait animation, effectively addressing these challenges. The adoption of a new video backbone model makes previous U-Net-based methods for identity maintenance, audio conditioning, and video extrapolation inapplicable. To address this limitation, we design an identity reference network consisting of a causal 3D VAE combined with a stacked series of transformer layers, ensuring consistent facial identity across video sequences. Additionally, we investigate various speech audio conditioning and motion frame mechanisms to enable the generation of continuous video driven by speech audio. Our method is validated through experiments on benchmark and newly proposed wild datasets, demonstrating substantial improvements over prior methods in generating realistic portraits characterized by diverse orientations within dynamic and immersive scenes. Further visualizations and the source code are available at: https://fudan-generative-vision.github.io/hallo3.

1. Introduction

Portrait image animation refers to the process of generating realistic facial expressions, lip movements, and head poses based on portrait images. This technique leverages various motion signals, including audio, textual prompts, facial keypoints, and dense motion flow. As a cross-disciplinary research task within the realms of computer vision and computer graphics, this area has garnered increasing attention from both academic and industrial communities. Furthermore, portrait image animation has critical applications across several sectors, including film and animation production, game development, social media content creation, and online education and training.

In recent years, the field of portrait image animation has witnessed rapid advancements. Early methodologies predominantly employed facial landmarks—key points [31, 43, 45] on the face utilized for the localization and representation of critical regions such as the mouth, eyes, eyebrows, nose, and jawline. Additionally, these methods [10, 26, 44, 51] incorporated 3D parametric models, notably the 3D Morphable Model (3DMM) [3], which captures variability in human faces through a statistical shape model integrated with a texture model. However, the application of explicit approaches grounded in intermediate facial representations is constrained by the accuracy of expression and head pose reconstruction, as well as the richness and precision of the resultant expressions. Simultaneously, significant advancements in Generative Adversarial Networks (GANs) and diffusion models have notably benefited portrait image animation. These advancements [7, 17, 35, 38, 40, 48, 51] enhance the high-resolution and high-quality generation of realistic facial details, facilitate generalized character animation, and enable long-term identity preservation. Recent contributions to the field—including Live Portrait [11], which leverages GAN technology for portrait animation with stitching and retargeting control, as well as various end-to-end methods such as VASA-1 [40], EMO [35], and Hallo [8, 39] employing diffusion models—exemplify these advancements.

Despite these improvements, existing methodologies encounter substantial limitations. First, many current facial animation techniques emphasize eye gaze, lip synchronization, and head posture while often depending on reference portrait images that present a frontal, centered view of the subject. This reliance presents challenges in handling profile, overhead, or low-angle perspectives for portrait animation. Secondly, accounting for significant accessories, such as holding a smartphone, microphone, or wearing closely fitted objects, presents challenges in generating realistic motion for the associated objects within video sequences.

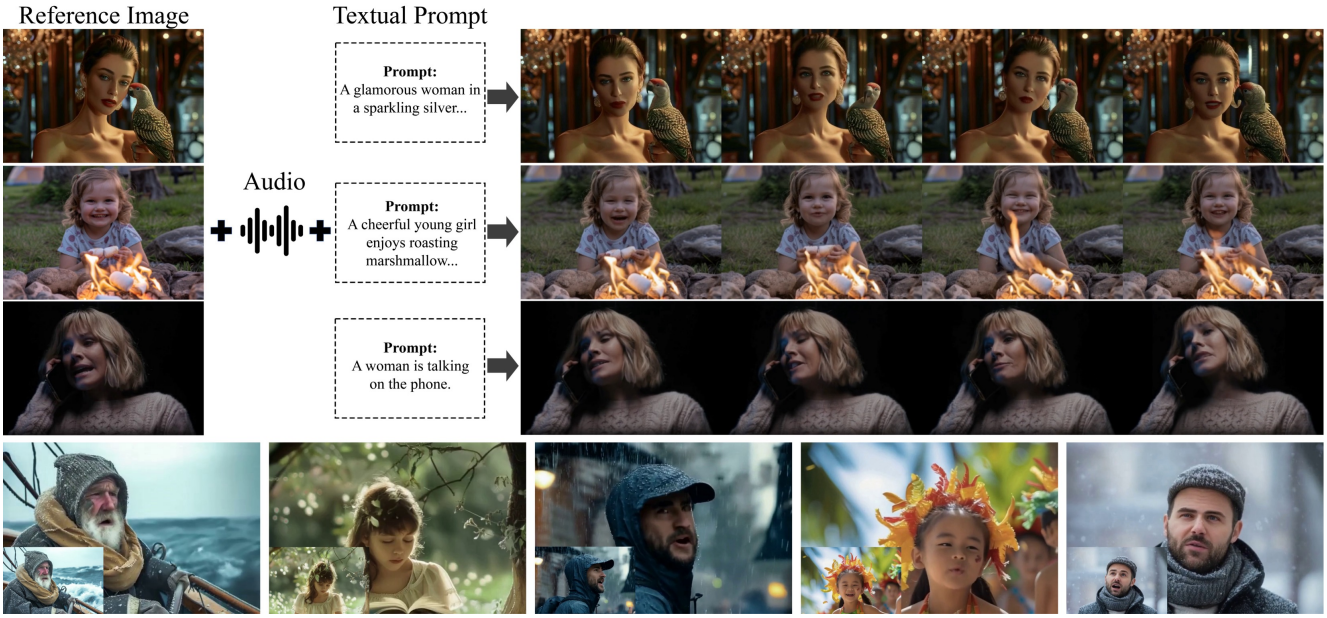

Figure 1. Demonstration of the proposed approach. Given a reference image, an audio sequence, and a textual prompt, the method generates animated portraits from frontal or different perspectives while preserving the portrait identity over extended durations. Additionally, it incorporates dynamic foreground and background elements, with temporal consistency and high visual fidelity.

Third, existing methods often assume static backgrounds, undermining their ability to generate authentic video effects in dynamic scenarios, such as those with campfires in the foreground or crowded street scenes in the background.

Recent advancements in diffusion transformer (DiT)-based video generation models [2,18,22,41] have addressed several challenges associated with traditional video generation techniques, including issues of realism, dynamic movement, and subject generalization. In this paper, we present the first application of a pretrained DiT-based video generative model to the task of portrait image animation. The introduction of this new video backbone model renders previous U-Net-based methods for identity maintenance, audio conditioning, and video extrapolation impractical. We tackle these issues from three distinct perspectives. (1) **Identity preservation**: We employ a 3D VAE in conjunction with a stack of transformer layers as an identity reference network, enabling the embedding and injection of identity information into the denoising latent codes for self-attention. This facilitates accurate representation and long-term preservation of the facial subject's identity. (2) **Speech audio conditioning**: We achieve high alignment between speech audio—serving as motion control information—and facial expression dynamics during training, which allows for precise control during inference. We investigate the use of adaptive layer normalization and cross-attention strategies, effectively integrating audio embeddings through the latter. (3) **Video extrapolation**: Addressing the limitations of the DiT-based model in generating continuous videos, which is constrained to a maximum of several tens of frames, we propose a strategy for long-duration video extrapolation. This approach uses motion frames as conditional information, wherein the final frames of each generated video serve as inputs for subsequent clip generation.

We validate our approach using benchmark datasets, including HTDF and Celeb-V, demonstrating results comparable to previous methods that are constrained to limited datasets characterized by frontal, centered faces, static backgrounds, and defined expressions. Furthermore, our method successfully generates dynamic foregrounds and backgrounds, accommodating complex poses, such as profile views or interactions involving devices like smartphones and microphones, yielding realistic and smoothly animated motion, thereby addressing challenges that previous methodologies have struggled to resolve effectively.

2. Related Work

Portrait Image Animation. Recent advancements in the domain of portrait image animation have been significantly propelled by innovations in audio-driven techniques. Notable frameworks, such as LipSyncExpert [23] and SadTalker [46], have tackled challenges related to facial synchronization and expression modulation, achieving dynamic lip movements and coherent head motions. Concurrently, DiffTalk [30] and VividTalk [33] have integrated latent diffusion models, enhancing output quality while generalizing across diverse identities without the necessity for extensive fine-tuning. Furthermore, studies

such as DreamTalk [19] and EMO [35] underscore the importance of emotional expressiveness by showcasing the integration of audio cues with facial dynamics. AniPortrait [38] and VASA-1 [40] propose methodologies that facilitate the generation of high-fidelity animations, emphasizing temporal consistency along with effective exploitation of static images and audio clips. In addition, recent innovations like LivePortrait [11] and Loopy [14] focus on enhancing computational efficiency while ensuring realism and fluid motion. Furthermore, the works of Hallo [39] and Hallo2 [8] have made significant progress in extending capabilities to facilitate long-duration video synthesis and integrating adjustable semantic inputs, thereby marking a step towards richer and more controllable content generation. Nevertheless, existing facial animation techniques still encounter limitations in addressing extreme facial poses, accommodating background motion in dynamic environments, and incorporating camera movements dictated by textual prompts.

Diffusion-Based Video Generation. Unet-based diffusion model has made notable strides, exemplified by frameworks such as Make-A-Video and MagicVideo [49]. Specifically, Make-A-Video [32] capitalizes on pre-existing Text-to-Image (T2I) models to enhance training efficiency without necessitating paired text-video data, thereby achieving state-of-the-art results across a variety of qualitative and quantitative metrics. Simultaneously, MagicVideo [49] employs an innovative 3D U-Net architecture to operate within a low-dimensional latent space, achieving efficient video synthesis while significantly reducing computational requirements. Building upon these foundational principles, AnimateDiff [12] introduces a motion module that integrates seamlessly with personalized T2I models, allowing for the generation of temporally coherent animations without the need for model-specific adjustments. Additionally, VideoComposer [37] enhances the controllability of video synthesis by incorporating spatial, temporal, and textual conditions, which facilitates improved inter-frame consistency. The development of diffusion models continues with the advent of DiT-based approaches such as CogVideoX [41] and Movie Gen [22]. CogVideoX employs a 3D Variational Autoencoder to improve video fidelity and narrative coherence, whereas Movie Gen establishes a robust foundation for high-quality video generation complemented by advanced editing capabilities. In the present study, we adopt the DiT diffusion formulation to optimize the generalization capabilities of the generated video.

3. Methodology

This methodology section systematically outlines the approaches employed in our study. Section 3.1 describes the baseline transformer diffusion network, detailing its architecture and functionality. Section 3.2 focuses on the integration of speech audio conditions via a cross-attention mechanism. Section 3.3 discusses the implementation of the identity reference network, which is crucial for preserving facial identity coherence throughout extended video sequences. Section 3.4 reviews the training and inference procedures used for the transformer diffusion network. Finally, Section 3.5 details the comprehensive strategies for data sourcing and preprocessing.

3.1. Baseline Transformer Diffusion Network

Baseline Network. The CogVideoX model [41] serves as the foundational architecture for our transformer diffusion network, employing a 3D VAE for the compression of video data. In this framework, latent variables are concatenated and reshaped into a sequential format, denoted as $\mathbf{z}_t$. Concurrently, the model utilizes the T5 architecture [24] to encode textual inputs into embeddings, represented as $\mathbf{c}_{\text{text}}$. The combined sequences of video latent representations $\mathbf{z}_t$ and textual embeddings $\mathbf{c}_{\text{text}}$ are subsequently processed through an expert transformer network. To address discrepancies in feature space between text and video, we implement expert adaptive layer normalization techniques, which facilitate the effective utilization of temporal information and ensure robust alignment between visual and semantic data. Following this integration, a repair mechanism is applied to restore the original latent variable, after which the output is decoded through the 3D causal VAE decoder to reconstruct the video. Furthermore, the incorporation of 3D Rotational Positional Encoding (3D RoPE) [41] enhances the model's capacity to capture inter-frame relationships across the temporal dimension, thereby establishing long-range dependencies within the video framework.

Conditioning in Diffusion Transformer. In addition to the textual prompt $\mathbf{c}_{\text{text}}$, we introduce two supplementary conditions: the speech audio condition $\mathbf{c}_{\text{audio}}$ and the identity appearance condition $\mathbf{c}_{\text{id}}$.

Within diffusion transformers, four primary conditioning mechanisms are identified: in-context conditioning, cross-attention, adaptive layer normalization (adaLN), and adaLN-zero [20]. Our investigation primarily focuses on cross-attention and adaptive layer normalization (adaLN). Cross-attention enhances the model's focus on conditional information by treating condition embeddings as keys and values, while latent representations serve as queries. Although adaLN is effective in simpler conditioning scenarios, it may not be optimal for more complex conditional embeddings that incorporate richer semantic details, such as sequential speech audio. Relevant comparative analyses will be elaborated upon in the experimental section.

3.2. Audio-Driven Transformer Diffusion

Speech Audio Embedding. To extract salient audio features for our proposed model, we utilize the wav2vec frame-

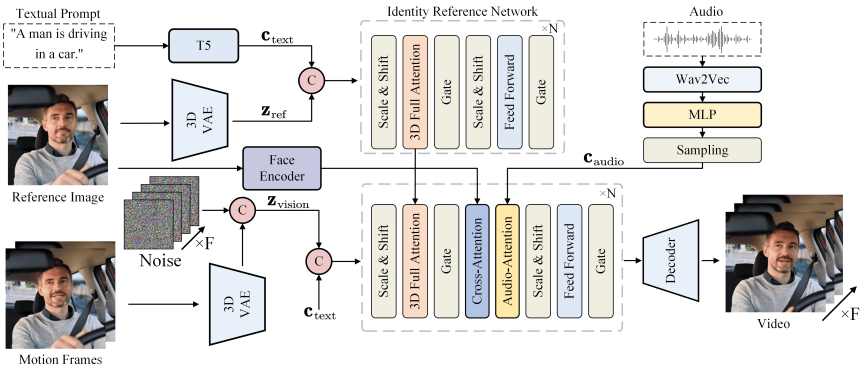

Figure 2. The overview of the proposed method. Specifically, the method takes a reference image, an audio sequence, and a textual prompt as inputs to generate a video output with temporal consistency and high visual fidelity. We leverage the casual 3D VAE, T5, and Wav2Vec models to process the visual, textual, and audio features, respectively. The Identity Reference Network extracts identity features from the input reference image and textual prompt, enabling controllable animation while preserving the subject's appearance. The audio encoder generates motion information for lip synchronization, while the face encoder extracts facial features to maintain consistency in facial expressions. The 3D Full Attention and Audio-Attention Modules combine identity and motion data within a denoising network, producing high-fidelity, temporally consistent, and controllable animated videos.

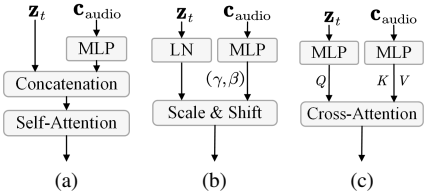

Figure 3. Different strategies of audio conditioning. (a) self-attention; (b) adaptive norm; (c) cross-attention.

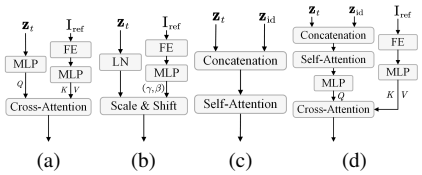

Figure 4. Different strategies of identity conditioning. FE refers to the face encoder. cross-attention demonstrates the best performance. (a) face attention; (b) face adaptive norm; (c) identity reference network; (d) face attention and identity reference network.

work developed by Schneider et al. [28]. The audio representation is defined as $\mathbf{c}_{\text{audio}}$. Specifically, we concatenate the audio embeddings generated by the final twelve layers of the wav2vec network, resulting in a comprehensive semantic representation capable of capturing various audio hierarchies. This concatenation emphasizes the significance of phonetic elements, such as pronunciation and prosody, which are crucial as driving signals for character generation. To transform the audio embeddings obtained from the pretrained model into frame-specific representations, we apply three successive linear transformation layers, mathematically expressed as: $\mathbf{c}_{\text{audio}}^{(f)} = \mathcal{L}_3\left(\mathcal{L}_2\left(\mathcal{L}_1\left(\mathbf{c}_{\text{audio}}\right)\right)\right)$, where $\mathcal{L}_1$, $\mathcal{L}_2$, and $\mathcal{L}_3$ represent the respective linear transformation functions. This systematic approach ensures that the resulting frame-specific representations effectively encapsulate the nuanced audio features essential for the performance of our model.

Speech Audio Conditioning. We explore three fusion strategies—self-attention, adaptive normalization, and cross-attention—as illustrated in Figure 3 to integrate audio condition into the DiT-based video generation model. Our experiments show that the cross-attention strategy delivers the best performance in our model. For more details, please refer to Section 4.3.

Following this, we integrate audio attention layers after each face-attention layer within the denoising network, employing a cross-attention mechanism that facilitates interaction between the latent encodings and the audio embeddings. Specifically, within the DiT block, the motion patches function as keys and values in the cross-attention computation with the hidden states $\mathbf{z}_t$: $\mathbf{z}_t = \text{CrossAttention}(\mathbf{z}_t, \mathbf{c}_{\text{audio}}^{(f)})$. This methodology leverages the conditional information from the audio embeddings to enhance the coherence and relevance of the generated outputs, ensuring that the model effectively captures the intricacies of the audio signals that drive character generation.

3.3. Identity Consistent Transformer Diffusion

Identity Reference Network. Diffusion transformer-based video generation models encounter significant challenges in maintaining facial identity coherence, particularly as the length of the generated video increases. While incorporating speech audio embeddings as conditional features can establish a correspondence between audio speech and facial movements, prolonged generation often leads to rapid degradation of facial identity characteristics.

To address this issue, we introduce a control condition within the existing diffusion transformer architecture to ensure long-term consistency of facial identity appearance. We explore four strategies (as shown in Figure 4) for appearance conditioning: 1) Face attention, where identity features are encoded by the face encoder and combined with a cross-attention module; 2) Face adaptive norm, which integrates features from the face encoder with an adaptive layer normalization technique; 3) Identity reference network, where identity features are captured by a 3D VAE and combined with some transformer layers; and 4) Face attention and Identity reference network, which encodes identity

features using both the face encoder and 3D VAE, combining them with self-attention and cross-attention. Our experiments show that the combination with Face attention and Identity reference net achieves the best performance in our model. For further details, please refer to Section 4.3.

We treat a reference image as a single frame and input it into a causal 3D VAE to obtain latent features, which are then processed through a reference network consisting of 42 transformer layers. Mathematically, if $\mathbf{I}_{\text{ref}}$ denotes the reference image, the encoder function of the 3D VAE is defined as: $\mathbf{z}_{\text{id}} = \mathcal{E}_{3D}(\mathbf{I}_{\text{ref}})$, where $\mathbf{z}_{\text{id}}$ represents the latent features associated with the reference image.

During the operation of the reference network, we extract vision tokens from the input of the 3D full attention mechanism for each transformer layer, which serve as reference features $\mathbf{z}_{\text{id}}$. These features are integrated into corresponding layers of the denoising network to enhance its capability, expressed as: $\mathbf{z}_{t,\text{enhanced}} = \text{SelfAttention}(\mathbf{z}_t, \mathbf{z}_{\text{id}})$, where $\mathbf{z}_t$ is the latent representation at time step t. Given that both the reference network and denoising network leverage the same causal 3D VAE with identical weights and comprise the same number of transformer layers (42 layers in our implementation), the visual features generated from both networks maintain semantic and scale consistency. This consistency allows the reference network's features to incorporate the appearance characteristics of facial identity from the reference image while minimizing disruption to the original feature representations of the denoising network, thereby reinforcing the model's capacity to generate coherent and identity-consistent facial animations across longer video sequences.

Temporal Motion Frames. To facilitate long video inference, we introduce the last n frames of the previously generated video, referred to as motion frames, as additional conditions. Given a generated video length of L and the corresponding latent representation of l frames, we denote the motion frames as N. The motion frames are processed through the 3D VAE to obtain n frames of latent codes. We apply zero padding to the subsequent $(l - n)$ frames and concatenate them with l frames of Gaussian noise. This concatenated representation is then patchified to yield vision tokens, which are subsequently input into the denoising network. By repeatedly utilizing motion frames, we achieve temporally consistent long video inference.

3.4. Training and Inference

Training. The training process consists of two phases:

(1) Identity Consistency Phase. In this initial phase, we train the model to generate videos with consistent identity. The parameters of the 3D Variational Autoencoder (VAE) and face image encoder remain fixed, while the parameters of the 3D full attention blocks in both the reference and denoising networks, along with the face attention blocks in the denoising network, are updated during training. The model's input includes a randomly sampled reference image from the training video, a textual prompt, and the face embedding. The textual prompt is generated using MiniCPM [42], which describes human appearance, actions, and detailed environmental background. The face embedding is extracted via InsightFace [9]. With these inputs, the model generates a video comprising 49 frames.

(2) Audio-Driven Video Generation Phase. In the second phase, we extend the training to include audio-driven video generation. We integrate audio attention modules into each transformer block of the denoising network, while fixing the parameters of other components and updating only those of the audio attention modules. Here, the model's input consists of a reference image, an audio embedding, and a textual prompt, resulting in a sequence of 49 video frames driven by audio.

Inference. During inference, the model receives a reference image, a segment of driving audio, a textual prompt, and motion frames as inputs. The model then generates a video that exhibits identity consistency and lip synchronization based on the driving audio. To produce long videos, we utilize the last two frames of the preceding video as motion frames, thereby achieving temporally consistent video generation.

3.5. Dataset

In this section, we will give a detailed introduction of our data curation, including data sources, filtering strategy and data statistics. Figure 5 shows the data pipeline and the statistical analysis of the final data.

Data Sources The training data used in this work is prepared from three distinct sources to ensure diversity and generalization. Specifically, the sources are: (1) HDTF dataset [47], which contains 8 hours of raw video footage; (2) YouTube data, which consists of 1,200 hours of public raw videos; (3) a large scale movie dataset, which contains film videos of 2,346 hours. Our dataset contains a large scale of human identities and, however, we find that YouTube and movie dataset contains a large amount of noised data. Therefore, we design a data curation pipeline as follows to construct a high-quality and diverse talking dataset, as shown in Figure 5(a).

Video Filtering. During the data pre-processing phase, we implement a series of meticulous filtering steps to ensure the quality and applicability of the dataset. The workflow includes three stages: extraction of single-speaker, motion filter and post-processing. Firstly, we select video of single-speaker. This stage aims to clean the video content to solve camera shot, background noise, etc, using existing tools [4, 21]. After that, we apply several filtering techniques to ensure the quality of head motion, head pose, camera motion, etc [6, 15, 16]. In this stage, we compute all

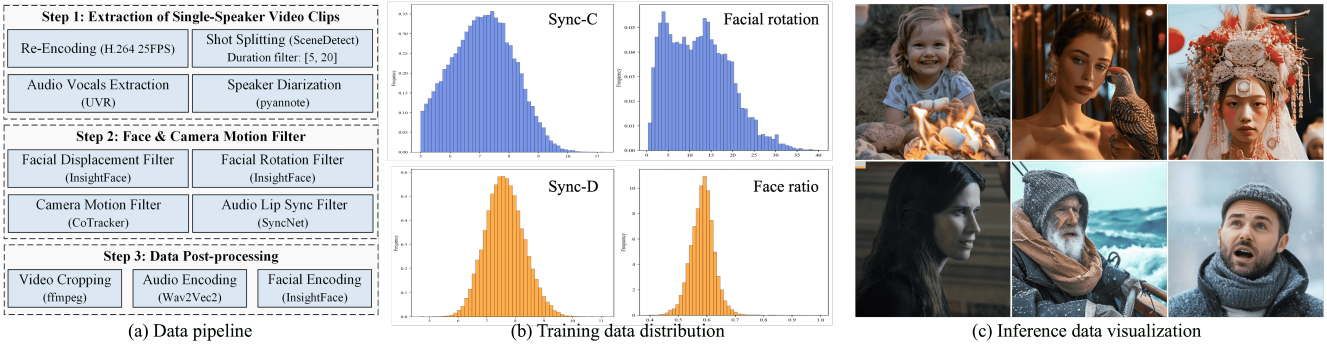

(a) Data pipeline (b) Training data distribution (c) Inference data visualization

Figure 5. Illustration of the dataset, including the flow of data processing, data distribution across different metric, and the visualization of some representative portrait images for inference.

metric scores for each clip, therefore, we can flexibly adjust data screening strategies to satisfy different data requirement of our multiple training stages or strategies. Finally, based on the facial positions detected in previous steps, we crop the videos to a 3:2 aspect ratio to meet the model's input requirements. We then select a random frame from each video and use InsightFace [25] to encode the face into embeddings, providing essential facial feature information for the model. Additionally, we extract the audio from the videos and encode it into embeddings using Wav2Vec2 model [1], facilitating the incorporation of audio conditions during model training.

Data Statistics. Following the data cleaning and filtering processes, we conducted a detailed analysis of the final dataset to assess its quality and suitability for the intended modeling tasks. Finally, our training data contains about 134 hours of videos, including 6 hours of high-quality data from HDTF dataset, 72 hours of YouTube videos, and 56 hours of movie videos. Figure 5(b) also shows other statistics, such as Lip Sync score (Sync-C and Sync-D), face rotation, face ratio (the ratio of face height to video height).

4. Experiment

4.1. Experimental Setups

Implementation. We initialize the identity reference and denoising networks with weights derived from CogVideoX-5B-I2V [41]. During both training phases, we employ the v-prediction diffusion loss [27] for optimization. Each training phase comprises 20,000 steps, utilizing 64 NVIDIA H100 GPUs. The batch size per GPU is set to 1, with a learning rate of 480×720 pixels. To enhance video generation variability, the reference image, guidance audio and textual prompt are dropped with a probability of 0.05 during training.

Evaluation Metrics. We employed a range of evaluation metrics for generated videos across benchmark datasets, including HDTF [47] and Celeb-V [50]. These metrics comprise Fréchet Inception Distance (FID) [29], Fréchet Video Distance (FVD) [36], Synchronization-C (Sync-C) [6], Synchronization-D (Sync-D) [6], and E-FID [35]. FID and FVD quantify the similarity between generated images and real data, while Sync-C and Sync-D assess lip synchronization accuracy. E-FID evaluates the image quality based on features extracted from the Inception network. Besides, we introduced VBench [13] metrics to enhance evaluation, focusing on dynamic degree and subject consistency. Dynamic degree is measured using RAFT [34] to quantify the extent of motion in generated videos, providing a comprehensive assessment of temporal quality. Subject consistency is measured through DINO [5] feature similarity, ensuring uniformity of a subject's appearance across frames.

Baseline Approaches. We considered several representative audio-driven talking face generation methods for comparison, all of which have publicly available source code or implementations. These methods include SadTalker [45], DreamTalk [19], AniPortrait [38], and Hallo [8, 39]. The selected approaches encompass both GANs and diffusion models, as well as techniques utilizing intermediate facial representations alongside end-to-end frameworks. This diversity in methodologies allows for a comprehensive evaluation of the effectiveness of our proposed approach compared to existing solutions.

4.2. Comparison with State-of-the-art

Comparison on HDTF and Celeb-V Dataset. As shown in Table 1 and 2, our method achieves best results on FID, FVD on both datasets. Although our approach shows some disparity compared to the state-of-the-art in lip synchronization, it still demonstrates promising results as illustrated in Figure 6. This is because, to generate animated portraits from different perspectives, our training data primarily consists of talking videos with significant head and body movements, as well as diverse dynamic scenes, unlike static scenes with minimal motion. While this may lead to some performance degradation on lip synchronization, it better reflects realistic application scenarios.

Comparison on Wild Dataset. To effectively demonstrate

	FID↓	FVD↓	Sync-C↑	Sync-D↓
SadTalker [45]	22.340	203.860	**7.885**	**7.545**
DreamTalk [19]	78.147	790.660	6.376	8.364
AniPortrait [38]	26.561	234.666	4.015	10.548
Hallo [39]	20.545	173.497	7.750	7.659
Ours	**20.359**	**160.838**	7.252	8.106
Real video	-	-	8.700	6.597

Table 1. Comparison with the other methods on HDTF dataset.

	FID↓	FVD↓	Sync-C↑	Sync-D↓	E-FID↓
SadTalker [45]	50.015	471.163	6.922	**7.921**	95.194
DreamTalk [19]	109.011	988.539	5.709	8.743	153.450
AniPortrait [38]	46.915	477.179	2.853	11.709	88.986
Hallo [39]	44.578	377.117	**7.191**	7.984	78.495
Ours	**43.271**	**355.272**	6.527	9.113	**71.210**
Real video	-	-	7.372	7.518	-

Table 2. Comparison with other methods on Celeb-V dataset.

	Sync-C↑	Sync-D↓	Subject Dynamic↑	Background Dynamic↑	Subject FVD↓	Background FVD↓
SadTalker [45]	3.845	10.378	2.953	0.220	470.377	313.758
DreamTalk [19]	4.498	11.005	6.958	1.806	835.480	744.177
AniPortrait [38]	1.685	12.025	3.351	1.769	473.173	302.716
Hallo [39]	4.654	10.202	5.268	1.272	394.627	291.052
Ours	**6.154**	**8.574**	**13.286**	**4.481**	**359.493**	**248.283**

Table 3. Comparison with other methods on our proposed wild dataset.

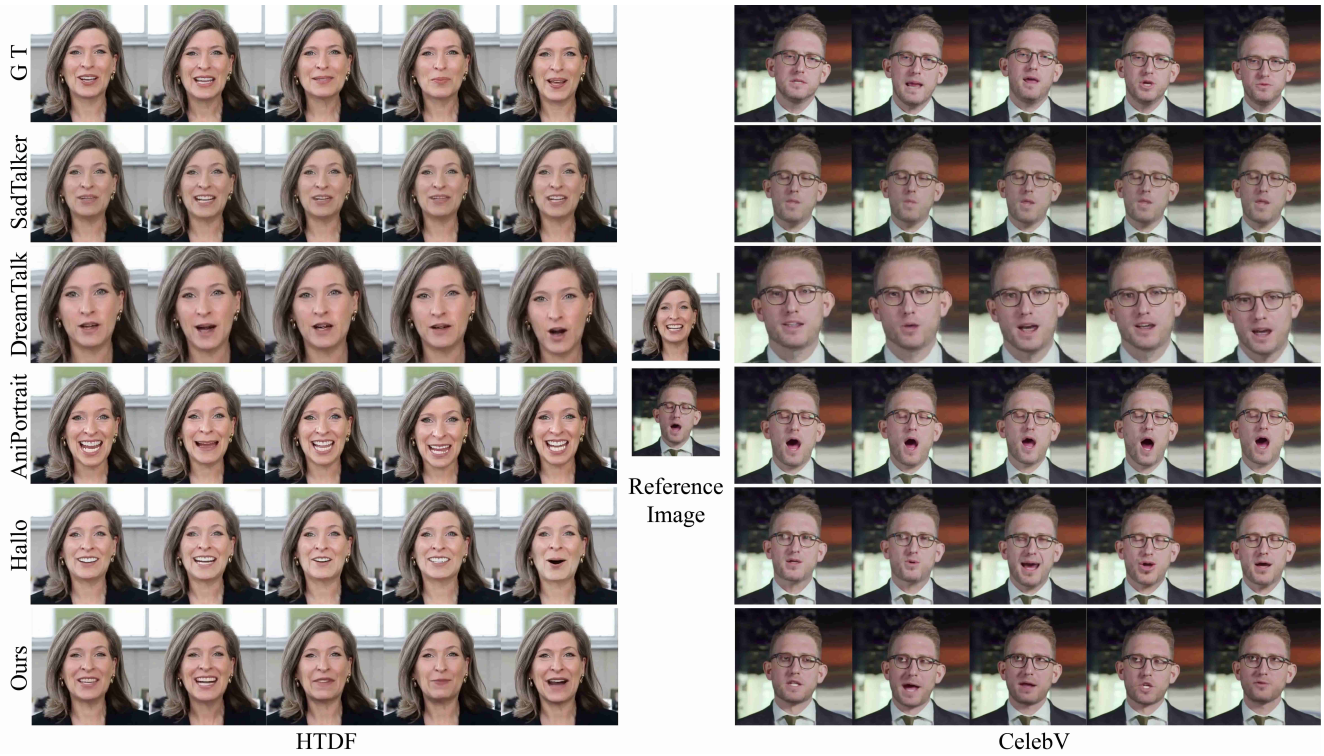

Figure 6. Qualitative comparison on the HTDF (left) and CelebV (right) data-set.

the performance of the general talking portrait video generation, we carefully collect 34 representative cases for evaluation. This dataset consists of portrait images with various head proportions, head poses, static and dynamic scenes and complex headwears and clothing. To achieve comprehensive assessment, we evaluate the performance on lip synchronization (Sync-C and Sync-D), motion strength (subject and background dynamic degree) and video quality (subject and background FVD). As shown in Table 3, our method generates videos with largest head and background dynamic degree (13.286 and 4.481) while keeping lip synchronization of highest accuracy.

Figure 7 provides a qualitative comparison of different portrait methods on a "wild" dataset. The results reveal that other methods struggle to animate side-face portrait images, often resulting in static poses or facial distortions. Additionally, these methods tend to focus solely on animating the face, overlooking interactions with other objects in the foreground—such as the dog next to the elderly, or the dynamic movement of the background—like the ostrich behind the girl. In contrast, as shown in Figure 8 our method produces realistic portraits with diverse orientations and complex foreground and background scenes.

4.3. Ablation Study and Discussion

Audio Conditioning. Table 4 and Figure 9 illustrate the effects of various strategies for incorporating audio conditioning. The results demonstrate that using cross-attention to integrate audio improves lip synchronization by enhancing the local alignment between visual and audio features, particularly around the lips. This is evident from the improvements in Sync-C and Sync-D, and it also contributes to a degree of enhancement in video quality.

Identity Reference Network. Table 5 and Figure 10 evaluate different identity conditioning strategies. The results indicate that without an identity condition, the model fails to preserve the portrait appearance. When using face embedding alone, the model introduces blur and distortion, as

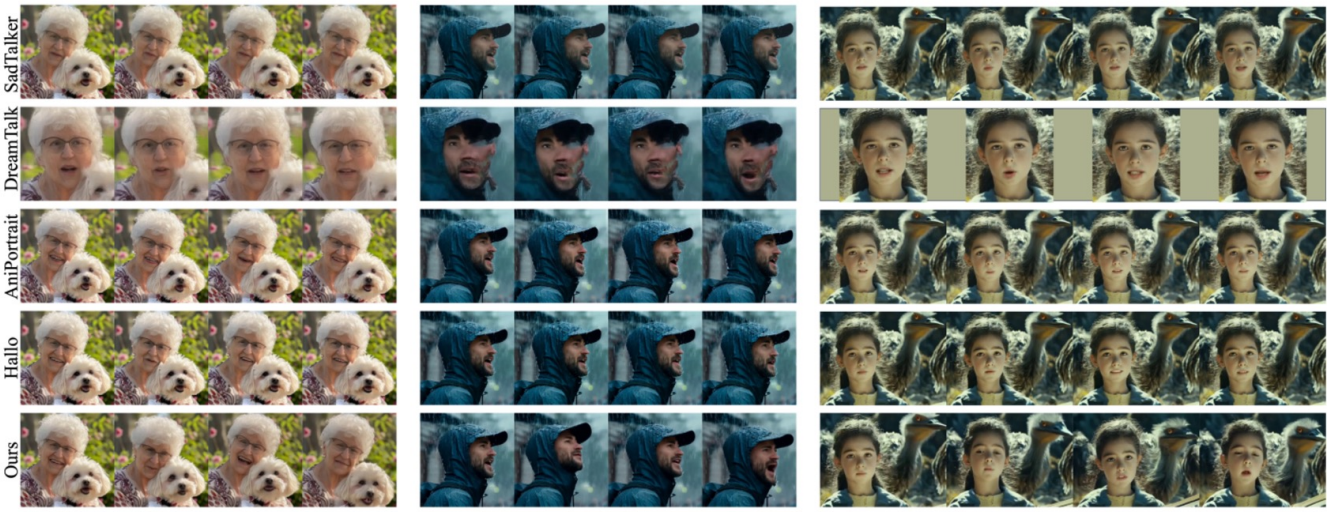

Figure 7. Complex facial identity with dynamic accessories subjects and different pose orientation.

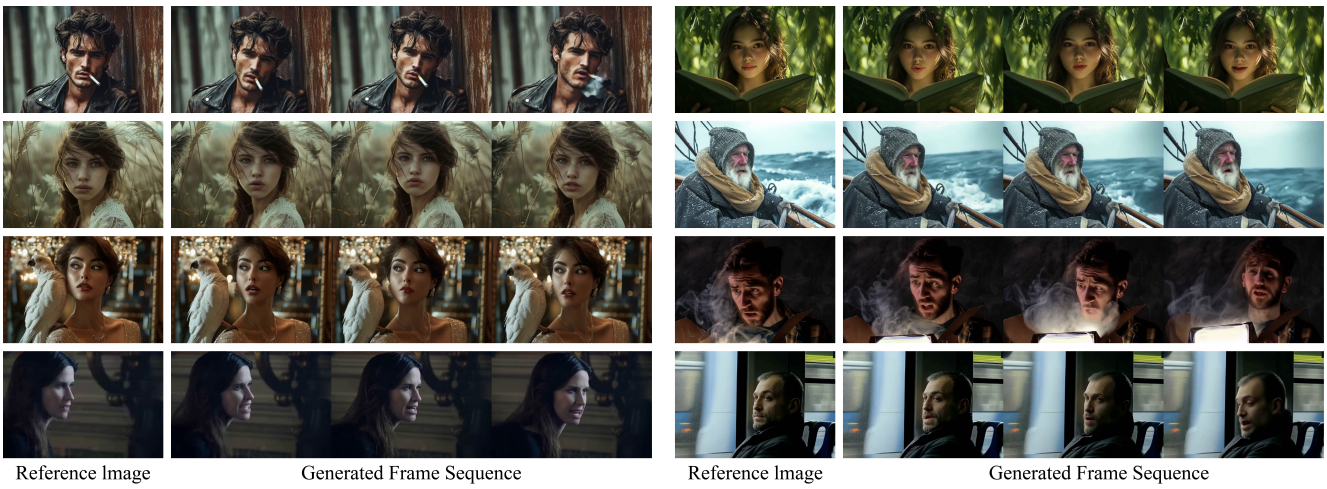

Figure 8. Complex scenes with dynamic foreground or background and various head poses.

it focuses solely on facial features and disrupts the global visual context. To address this, we introduce an identity reference network to preserve global features while making facial motion more controllable through identity-based facial embeddings. Thus, the proposed method achieves a lower FID of 23.458 and FVD of 242.602, while maintaining lip synchronization.

Temporal Motion Frames. Table 6 presents an analysis of varying temporal motion frames. One motion frame achieves the highest Sync-C score (6.889) and the lowest Sync-D score (8.695), indicating substantial lip synchronization.

CFG Scales for Diffusion Model. Table 7 provides a quantitative analysis of video generations using various CFG scales for audio, text, and reference images. A comparison between the second and fourth rows demonstrates that increasing the audio CFG scale enhances the model's ability to synchronize lip movements. The text CFG scale significantly influences the video's dynamism, as indicated in the first three rows, where both the subject's and the background's dynamics increase with higher text CFG scales. Conversely, the reference image CFG scale primarily governs the subject's appearance; higher values improve subject consistency, as illustrated by the second and fifth rows. Among the tested configurations, setting $\lambda_a = 3.5$, $\lambda_t = 3.5$, and $\lambda_i = 1.0$ yields a balanced performance. This interplay between visual fidelity and dynamics underscores the effectiveness of CFG configurations in generating realistic portrait animations.

Limitations and Future Works. Despite the advancements in portrait image animation techniques presented in this study, several limitations warrant acknowledgment. While

Figure 9. Qualitative comparison of different strategies for audio conditioning.

Audio Injection Method	FID↓	FVD↓	Sync-C↑	Sync-D↓
adaLN	24.159	264.331	1.374	13.524
adaLN-zero	24.029	276.403	1.398	13.553
Self Attn.	24.748	270.101	1.345	13.456
Cross Attn. (Ours)	**23.458**	**242.602**	**4.601**	**10.416**

Table 4. Comparison on the different strategy of audio conditioning.

Identity Injection Method	FID↓	FVD↓	Sync-C↑	Sync-D↓	Subject Consistency↑
(a) No identity condition	32.304	371.820	3.183	11.732	0.977
(b) Face attention	57.541	740.536	4.042	10.682	0.974
(c) Face adaptive norm	150.720	1587.395	3.822	12.324	0.904
(d) Identity reference network	28.789	291.863	4.553	**10.317**	0.984
(e) Face attention and Identity reference network	**23.458**	**242.602**	**4.601**	10.416	**0.988**

Table 5. Comparison of different identity injection method. "No identity condition" refers to the absence of any conditioning related to identity; "Face attention" and "Face adaptive norm" involve incorporating face embeddings using self-attention and adaptive layer normalization, respectively. "Identity reference network" refers to the introduction of identity features using a reference network.

Motion Frame Number	FID↓	FVD↓	Sync-C↑	Sync-D↓
n = 1	24.040	242.708	**6.889**	**8.695**
n = 2	**23.458**	**242.602**	4.601	10.416
n = 4	24.459	269.904	5.109	10.489
n = 8	27.303	265.396	5.114	10.464

Table 6. Ablation on the number of motion frames.

the proposed methods improve identity preservation and lip synchronization, the model's ability to realistically represent intricate facial expressions in dynamic environments still requires refinement, especially under varying illumination conditions. Future work will focus on enhancing the model's robustness to diverse perspectives and interactions, incorporating more comprehensive datasets that include varied backgrounds and facial accessories. Furthermore, investigating the integration of real-time feedback mechanisms could significantly enhance the interactivity and realism of portrait animations, paving the way for broader applications in live media and augmented reality.

Safety Considerations. The advancement of portrait image animation technologies, particularly those driven by audio inputs, presents several social risks, most notably concerning the ethical implications associated with the creation of highly realistic portraits that may be misused for deepfake purposes. To address these concerns, it is essential to develop comprehensive ethical guidelines and responsible use practices. Moreover, issues surrounding privacy and consent are prominent when utilizing individuals' images and voices. It is imperative to establish transparent data usage policies, ensuring that individuals provide informed consent and that their privacy rights are fully protected. By acknowledging these risks and implementing appropriate mitigation strategies, this research aims to promote the responsible and ethical development of portrait image animation technology.

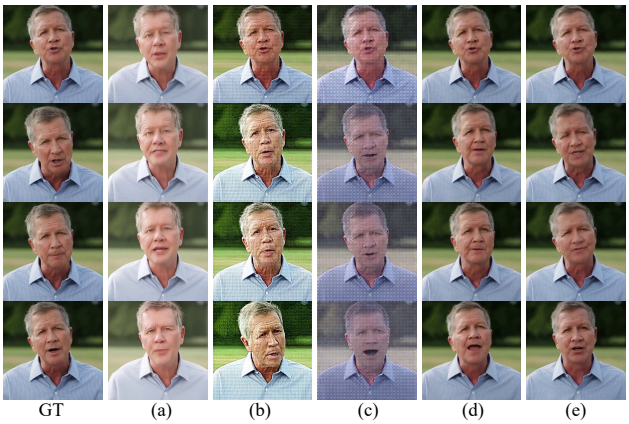

Figure 10. Qualitative comparison of different strategies (as in Table 5) for identity conditioning. (a) No identity condition; (b) Face attention; (c) Face adaptive norm; (d) Identity reference network; (e) Face attention and Identity reference network.

4.4. Generation Controllability

Textual Prompt for Subject Animation. To evaluate whether textual conditional controllability is effectively preserved, we conducted a series of experiments comparing the performance of our method to that of the baseline model, CogVideoX [41], using same text prompts. As shown in Figure 11, the results shows that our model maintains its ability for textual control, and effectively captures the interaction between different subjects as dictated by the textual prompts.

Textual Prompt for Foreground and Background Animation. We also explore model's ability to follow the foreground and background textual prompt. As illustrated in Figure 12, our method animates the foreground and background subjects naturally, such as the ocean waves and flickering candlelight. The results demonstrates the model's ability to control foreground, and background with the textual caption, which is maintained even after introducing the audio condition.

	Audio	Text	Image	Sync-C↑	Sync-D↓	Subject Dynamic↑	Background Dynamic↑	Subject FVD↓	Background FVD↓	Subject Consistency↑
$\lambda_t \downarrow$	$\lambda_a = 3.5$	$\lambda_t = 1.0$	$\lambda_i = 1.0$	6.168	8.589	13.164	3.955 ↓	361.582	263.416	0.9813
Base	$\lambda_a = 3.5$	$\lambda_t = 3.5$	$\lambda_i = 1.0$	6.154	8.574	13.286	4.481	359.493	248.283	0.9810
$\lambda_t \uparrow$	$\lambda_a = 3.5$	$\lambda_t = 6.0$	$\lambda_i = 1.0$	6.044	8.861	13.616	4.659 ↑	342.894	235.307	0.9808
$\lambda_a \uparrow$	$\lambda_a = 6.0$	$\lambda_t = 3.5$	$\lambda_i = 1.0$	6.469 ↑	8.515	14.778	4.066	379.073	264.969	0.9809
$\lambda_i \uparrow$	$\lambda_a = 3.5$	$\lambda_t = 3.5$	$\lambda_i = 3.5$	6.023	8.654	12.599	4.219	367.225	265.414	0.9835 ↑

Table 7. Quantitative study of audio, text and image CFG scales on our proposed wild dataset.

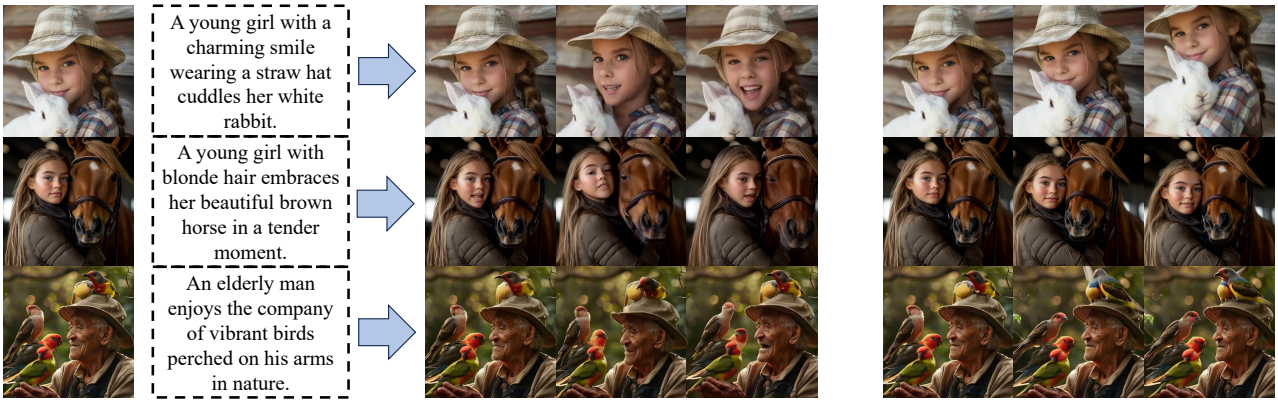

Figure 11. Condition on interacting with subjects. Our method achieves alignment comparable to that of CogVideX, maintaining the controllability of interactive subjects even after introducing the audio condition.

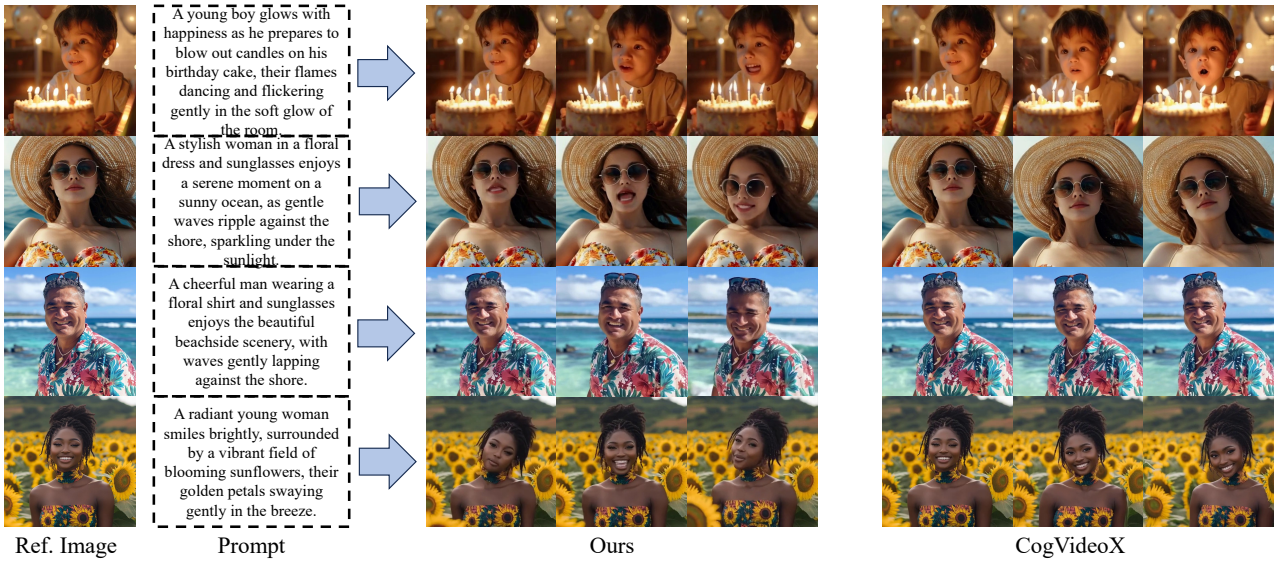

Figure 12. Textual condition on foreground and background. Our method achieves alignment comparable to that of CogVideX, maintaining the controllability of foreground and background after incorporating the audio condition.

5. Conclusion

This paper introduces advancements in portrait image animation utilizing the enhanced capabilities of a transformer-based diffusion model. By integrating audio conditioning through cross-attention mechanisms, our approach effectively captures the intricate relationship between audio signals and facial expressions, achieving substantial lip synchronization. To preserve facial identity across video sequences, we incorporate an identity reference network. Additionally, we utilize motion frames to enable the model to generate long-duration video extrapolations. Our model produces animated portraits from diverse perspectives, seamlessly blending dynamic foreground and background elements while maintaining temporal consistency and high fidelity.

References

[1] Alexei Baevski, Yuhao Zhou, Abdelrahman Mohamed, and Michael Auli. wav2vec 2.0: A framework for self-supervised learning of speech representations. Advances in neural information processing systems, 33:12449–12460, 2020. 6

[2] Fan Bao, Chendong Xiang, Gang Yue, Guande He, Hongzhou Zhu, Kaiwen Zheng, Min Zhao, Shilong Liu, Yaole Wang, and Jun Zhu. Vidu: a highly consistent, dynamic and skilled text-to-video generator with diffusion models. arXiv preprint arXiv:2405.04233, 2024. 2

[3] Volker Blanz and Thomas Vetter. Face recognition based on fitting a 3d morphable model. IEEE Transactions on pattern analysis and machine intelligence, 25(9):1063–1074, 2003. 1

[4] Hervé Bredin. pyannote.audio 2.1 speaker diarization pipeline: principle, benchmark, and recipe. In Proc. INTERSPEECH 2023, 2023. 5

[5] Mathilde Caron, Hugo Touvron, Ishan Misra, Hervé Jégou, Julien Mairal, Piotr Bojanowski, and Armand Joulin. Emerging properties in self-supervised vision transformers. In Proceedings of the International Conference on Computer Vision (ICCV), 2021. 6

[6] J. S. Chung and A. Zisserman. Out of time: automated lip sync in the wild. In Workshop on Multi-view Lip-reading, ACCV, 2016. 5, 6

[7] Enric Corona, Andrei Zanfir, Eduard Gabriel Bazavan, Nikos Kolotouros, Thiemo Alldieck, and Cristian Sminchisescu. Vlogger: Multimodal diffusion for embodied avatar synthesis. arXiv preprint arXiv:2403.08764, 2024. 1

[8] Jiahao Cui, Hui Li, Yao Yao, Hao Zhu, Hanlin Shang, Kaihui Cheng, Hang Zhou, Siyu Zhu, and Jingdong Wang. Hallo2: Long-duration and high-resolution audio-driven portrait image animation. arXiv preprint arXiv:2410.07718, 2024. 1, 3, 6

[9] DeepInsight. Insightface: An open-source 2d and 3d deep face analysis toolkit. https://github.com/deepinsight/insightface, 2024. 5

[10] Yue Gao, Yuan Zhou, Jinglu Wang, Xiao Li, Xiang Ming, and Yan Lu. High-fidelity and freely controllable talking head video generation. In Proceedings of the IEEE/CVF Conference on Computer Vision and Pattern Recognition (CVPR), pages 5609–5619, 2023. 1

[11] Jianzhu Guo, Dingyun Zhang, Xiaoqiang Liu, Zhizhou Zhong, Yuan Zhang, Pengfei Wan, and Di Zhang. Liveportrait: Efficient portrait animation with stitching and retargeting control. arXiv preprint arXiv:2407.03168, 2024. 1, 3

[12] Yuwei Guo, Ceyuan Yang, Anyi Rao, Yaohui Wang, Yu Qiao, Dahua Lin, and Bo Dai. Animatediff: Animate your personalized text-to-image diffusion models without specific tuning. arXiv preprint arXiv:2307.04725, 2023. 3

[13] Ziqi Huang, Yinan He, Jiashuo Yu, Fan Zhang, Chenyang Si, Yuming Jiang, Yuanhan Zhang, Tianxing Wu, Qingyang Jin, Nattapol Chanpaisit, Yaohui Wang, Xinyuan Chen, Limin Wang, Dahua Lin, Yu Qiao, and Ziwei Liu. VBench: Comprehensive benchmark suite for video generative models. In Proceedings of the IEEE/CVF Conference on Computer Vision and Pattern Recognition, 2024. 6

[14] Jianwen Jiang, Chao Liang, Jiaqi Yang, Gaojie Lin, Tianyun Zhong, and Yanbo Zheng. Loopy: Taming audio-driven portrait avatar with long-term motion dependency. arXiv preprint arXiv:2409.02634, 2024. 3

[15] Nikita Karaev, Iurii Makarov, Jianyuan Wang, Natalia Neverova, Andrea Vedaldi, and Christian Rupprecht. Cotracker3: Simpler and better point tracking by pseudo-labelling real videos. In Proc. arXiv:2410.11831, 2024. 5

[16] Nikita Karaev, Ignacio Rocco, Benjamin Graham, Natalia Neverova, Andrea Vedaldi, and Christian Rupprecht. Cotracker: It is better to track together. In Proc. ECCV, 2024. 5

[17] Tao Liu, Feilong Chen, Shuai Fan, Chenpeng Du, Qi Chen, Xie Chen, and Kai Yu. Anitalker: Animate vivid and diverse talking faces through identity-decoupled facial motion encoding. arXiv preprint arXiv:2405.03121, 2024. 1

[18] Yixin Liu, Kai Zhang, Yuan Li, Zhiling Yan, Chujie Gao, Ruoxi Chen, Zhengqing Yuan, Yue Huang, Hanchi Sun, Jianfeng Gao, et al. Sora: A review on background, technology, limitations, and opportunities of large vision models. arXiv preprint arXiv:2402.17177, 2024. 2

[19] Yifeng Ma, Shiwei Zhang, Jiayu Wang, Xiang Wang, Yingya Zhang, and Zhidong Deng. Dreamtalk: When expressive talking head generation meets diffusion probabilistic models. arXiv preprint arXiv:2312.09767, 2023. 3, 6, 7

[20] William Peebles and Saining Xie. Scalable diffusion models with transformers. In Proceedings of the IEEE/CVF International Conference on Computer Vision (ICCV), pages 4195–4205, 2023. 3

[21] Alexis Plaquet and Hervé Bredin. Powerset multi-class cross entropy loss for neural speaker diarization. In Proc. INTERSPEECH 2023, 2023. 5

[22] Adam Polyak, Amit Zohar, Andrew Brown, Andros Tjandra, Animesh Sinha, Ann Lee, Apoorv Vyas, Bowen Shi, Chih-Yao Ma, Ching-Yao Chuang, et al. Movie gen: A cast of media foundation models. arXiv preprint arXiv:2410.13720, 2024. 2, 3

[23] KR Prajwal, Rudrabha Mukhopadhyay, Vinay P Namboodiri, and CV Jawahar. A lip sync expert is all you need for speech to lip generation in the wild. In Proceedings of the 28th ACM international conference on multimedia (ACM MM), pages 484–492, 2020. 2

[24] Colin Raffel, Noam Shazeer, Adam Roberts, Katherine Lee, Sharan Narang, Michael Matena, Yanqi Zhou, Wei Li, and Peter J. Liu. Exploring the limits of transfer learning with a unified text-to-text transformer, 2023. 3

[25] Xingyu Ren, Alexandros Lattas, Baris Gecer, Jiankang Deng, Chao Ma, and Xiaokang Yang. Facial geometric detail recovery via implicit representation. In 2023 IEEE 17th International Conference on Automatic Face and Gesture Recognition (FG), 2023. 6

[26] Yurui Ren, Ge Li, Yuanqi Chen, Thomas H Li, and Shan Liu. Pirenderer: Controllable portrait image generation via semantic neural rendering. In Proceedings of the IEEE/CVF International Conference on Computer Vision (ICCV), pages 13759–13768, 2021. 1

[27] Tim Salimans and Jonathan Ho. Progressive distillation for fast sampling of diffusion models. arXiv preprint arXiv:2202.00512, 2022. 6

[28] Steffen Schneider, Alexei Baevski, Ronan Collobert, and Michael Auli. wav2vec: Unsupervised pre-training for speech recognition. arXiv preprint arXiv:1904.05862, 2019. 4

[29] Maximilian Seitzer. pytorch-fid: FID Score for PyTorch. https://github.com/mseitzer/pytorch-fid, August 2020. Version 0.3.0. 6

[30] Shuai Shen, Wenliang Zhao, Zibin Meng, Wanhua Li, Zheng Zhu, Jie Zhou, and Jiwen Lu. Difftalk: Crafting diffusion models for generalized audio-driven portraits animation. In Proceedings of the IEEE/CVF Conference on Computer Vision and Pattern Recognition, pages 1982–1991, 2023. 2

[31] Aliaksandr Siarohin, Stéphane Lathuilière, Sergey Tulyakov, Elisa Ricci, and Nicu Sebe. First order motion model for image animation. Advances in Neural Information Processing Systems (NeurIPS), 32, 2019. 1

[32] Uriel Singer, Adam Polyak, Thomas Hayes, Xi Yin, Jie An, Songyang Zhang, Qiyuan Hu, Harry Yang, Oron Ashual, Oran Gafni, et al. Make-a-video: Text-to-video generation without text-video data. arXiv preprint arXiv:2209.14792, 2022. 3

[33] Xusen Sun, Longhao Zhang, Hao Zhu, Peng Zhang, Bang Zhang, Xinya Ji, Kangneng Zhou, Daiheng Gao, Liefeng Bo, and Xun Cao. Vividtalk: One-shot audio-driven talking head generation based on 3d hybrid prior. arXiv preprint arXiv:2312.01841, 2023. 2

[34] Zachary Teed and Jia Deng. Raft: Recurrent all-pairs field transforms for optical flow. In Computer Vision–ECCV 2020: 16th European Conference, Glasgow, UK, August 23–28, 2020, Proceedings, Part II 16, pages 402–419. Springer, 2020. 6

[35] Linrui Tian, Qi Wang, Bang Zhang, and Liefeng Bo. Emo: Emote portrait alive-generating expressive portrait videos with audio2video diffusion model under weak conditions. arXiv preprint arXiv:2402.17485, 2024. 1, 3, 6

[36] Thomas Unterthiner, Sjoerd van Steenkiste, Karol Kurach, Raphael Marinier, Marcin Michalski, and Sylvain Gelly. Towards accurate generative models of video: A new metric & challenges. arXiv preprint arXiv:1812.01717, 2018. 6

[37] Xiang Wang, Hangjie Yuan, Shiwei Zhang, Dayou Chen, Jiuniu Wang, Yingya Zhang, Yujun Shen, Deli Zhao, and Jingren Zhou. Videocomposer: Compositional video synthesis with motion controllability. Advances in Neural Information Processing Systems (NeurIPS), 36, 2024. 3

[38] Huawei Wei, Zejun Yang, and Zhisheng Wang. Aniportrait: Audio-driven synthesis of photorealistic portrait animation. arXiv preprint arXiv:2403.17694, 2024. 1, 3, 6, 7

[39] Mingwang Xu, Hui Li, Qingkun Su, Hanlin Shang, Liwei Zhang, Ce Liu, Jingdong Wang, Yao Yao, and Siyu zhu. Hallo: Hierarchical audio-driven visual synthesis for portrait image animation, 2024. 1, 3, 6, 7

[40] Sicheng Xu, Guojun Chen, Yu-Xiao Guo, Jiaolong Yang, Chong Li, Zhenyu Zang, Yizhong Zhang, Xin Tong, and Baining Guo. Vasa-1: Lifelike audio-driven talking faces generated in real time. arXiv preprint arXiv:2404.10667, 2024. 1, 3

[41] Zhuoyi Yang, Jiayan Teng, Wendi Zheng, Ming Ding, Shiyu Huang, Jiazheng Xu, Yuanming Yang, Wenyi Hong, Xiaohan Zhang, Guanyu Feng, et al. Cogvideox: Text-to-video diffusion models with an expert transformer. arXiv preprint arXiv:2408.06072, 2024. 2, 3, 6, 9

[42] Yuan Yao, Tianyu Yu, Ao Zhang, Chongyi Wang, Junbo Cui, Hongji Zhu, Tianchi Cai, Haoyu Li, Weilin Zhao, Zhihui He, et al. Minicpm-v: A gpt-4v level mllm on your phone. arXiv preprint arXiv:2408.01800, 2024. 5

[43] Egor Zakharov, Aleksei Ivakhnenko, Aliaksandra Shysheya, and Victor Lempitsky. Fast bi-layer neural synthesis of one-shot realistic head avatars. In Computer Vision–ECCV 2020: 16th European Conference, Glasgow, UK, August 23–28, 2020, Proceedings, Part XII 16, pages 524–540. Springer, 2020. 1

[44] Bowen Zhang, Chenyang Qi, Pan Zhang, Bo Zhang, Hsiang-Tao Wu, Dong Chen, Qifeng Chen, Yong Wang, and Fang Wen. Metaportrait: Identity-preserving talking head generation with fast personalized adaptation. In Proceedings of the IEEE/CVF Conference on Computer Vision and Pattern Recognition (CVPR), pages 22096–22105, 2023. 1

[45] Wenxuan Zhang, Xiaodong Cun, Xuan Wang, Yong Zhang, Xi Shen, Yu Guo, Ying Shan, and Fei Wang. Sadtalker: Learning realistic 3d motion coefficients for stylized audio-driven single image talking face animation. In Proceedings of the IEEE/CVF Conference on Computer Vision and Pattern Recognition (CVPR), pages 8652–8661, 2023. 1, 6, 7

[46] Wenxuan Zhang, Xiaodong Cun, Xuan Wang, Yong Zhang, Xi Shen, Yu Guo, Ying Shan, and Fei Wang. Sadtalker: Learning realistic 3d motion coefficients for stylized audio-driven single image talking face animation. In Proceedings of the IEEE/CVF Conference on Computer Vision and Pattern Recognition (CVPR), pages 8652–8661, 2023. 2

[47] Zhimeng Zhang, Lincheng Li, Yu Ding, and Changjie Fan. Flow-guided one-shot talking face generation with a high-resolution audio-visual dataset. In Proceedings of the IEEE/CVF Conference on Computer Vision and Pattern Recognition, pages 3661–3670, 2021. 5, 6

[48] Zhenghao Zhang, Junchao Liao, Menghao Li, Long Qin, and Weizhi Wang. Tora: Trajectory-oriented diffusion transformer for video generation. arXiv preprint arXiv:2407.21705, 2024. 1

[49] Daquan Zhou, Weimin Wang, Hanshu Yan, Weiwei Lv, Yizhe Zhu, and Jiashi Feng. Magicvideo: Efficient video generation with latent diffusion models. arXiv preprint arXiv:2211.11018, 2022. 3

[50] Hao Zhu, Wayne Wu, Wentao Zhu, Liming Jiang, Siwei Tang, Li Zhang, Ziwei Liu, and Chen Change Loy. CelebV-HQ: A large-scale video facial attributes dataset. In ECCV, 2022. 6

[51] Shenhao Zhu, Junming Leo Chen, Zuozhuo Dai, Yinghui Xu, Xun Cao, Yao Yao, Hao Zhu, and Siyu Zhu. Champ: Controllable and consistent human image animation with 3d parametric guidance, 2024. 1